J Ther Eng, Vol. 11, No. 2, pp. 508−518, March, 2025

Journal of Thermal Engineering
Web page info: https://jten.yildiz.edu.tr
DOI: 10.14744/thermal.0000930

Research Article

Performance improvement of a decayed flow heat exchanger using spiral flow and nanofluid

Walaa M. HASHIM[1,*], Faten N. AL-ZUBAIDI[1], Huda A. AL-SALIHI[1]

[1]*Department of Electromechanical Engineering, University of Technology, Baghdad, 10066, Iraq*

ARTICLE INFO

Article history
Received: 07 August 2023
Revised: 29 March 2024
Accepted: 07 April 2024

Keywords:
Decayed Flow and Nanofluid; Heat Exchanger; Spiral Flow; Swirl; Taylor Vortex

ABSTRACT

The demand for heat exchangers that have high performance is still a major challenge for the industrial field. In this work, a spiral flow of cold air and a 0.5% volume concentration of the nanoaluminum metal heat exchanger were used to analyze the Taylor vortex that forms in the hot nanofluid Al_2O_3. According to the experimental results, the effectiveness of the heat exchanger at the ratio C_{min}/C_{max} of 0.08 could be improved over that of the exchanger at the ratio C_{min}/C_{max} of 0.0. Additionally, at an inner cylinder rotational speed of 80 r.p.m, employing the spiral flow of cold air and nanofluid as a hot fluid to transfer heat increased its efficacy can reach up to 53.8%.

Cite this article as: Hashim WM, Al-Zubaidi FN, Al-Salihi HA. Performance improvement of a decayed flow heat exchanger using spiral flow and nanofluid. J Ther Eng 2025;11(2):508−518.

INTRODUCTION

In terms of energy conversion, it is important to enhance the thermal performance of heat exchangers. Heat exchanger efficiency is often determined by the amount of heat transfer, which should be kept to a maximum depending on their size. One possible way to improve the rate of heat transfer in a spiral tube heat exchanger is by creating vortices and using nanofluids as a working medium. As a result, there is a significant increase in the quantity of heat transmitted through the exchanger [1]. Nanofluids are particularly effective at increasing heat transfer and typically have a higher thermal conductivity than other conventional fluids. Infinite spiral flow is an alternative method to extend the time needed for working fluid heat transfer through exchangers [2-9] and employing a high-conductivity heat transfer medium.

An example of a heat exchanger that uses a spiral flow channel to transfer heat from one working fluid to another is a spiral heat exchanger. The fluids flow in opposite directions through the spiral channels. The spiral form of the channels increases the surface area for heat transfer as well as contributes to the turbulent flow, which improves the efficiency of a heat exchanger. The compact design of spiral heat exchangers makes them ideal for applications like power plants, nuclear reactors, steam generation, air-conditioning systems, heat recovery units, and chemical processing where space is limited. Taylor-Couette flow, on the other hand, is a well-known flow between coaxial cylinders with the inner cylinder rotating. This unusual flow has recently been used in the processing of food. Gelatinization

***Corresponding author.**
*E-mail address: 50091@uotechnology.edu.iq

This paper was recommended for publication in revised form by Editor-in-Chief Ahmet Selim Dalkılıç

Published by Yıldız Technical University Press, İstanbul, Turkey
Copyright 2021, Yıldız Technical University. This is an open access article under the CC BY-NC license (http://creativecommons.org/licenses/by-nc/4.0/).

in the starch processing process is greatly enhanced by better heat transfer through Taylor vortex flow.

Hashim et al. [10] investigated the Taylor vortex produced in the hot water flow of the smooth surface heat exchanger while a swirl flow occurred in cool air. Another attempt was made to improve the outcome by using nanoaluminum metal for the heat transfer surface. According to the experimental data, heat exchanger effectiveness at the ratio (C_{min}/C_{max} = 0.08) might be improved above conventional exchanger efficiency at the ratio (C_{min}/C_{max} = 0).

Previous research [10] found that using nanoaluminum as the working medium increased heat transfer efficiency by 3,2%, 4,3%, and 4,58% for inner cylinder rotational speeds of 0, 65, and 80 r.p.m.

Onyiriuka et al. [11] quantitatively modeled the heat transfer characteristics of a new type of nanofluid made from mango bark in a double-pipe heat exchanger utilizing turbulent flow. The current study looked at different volume percentages with particle sizes of 100 nm. It was discovered that Nusselt's number increased by 68% when Reynolds number was 5000 but only by 45% when Reynolds number was 13000. Additionally, it was discovered that the Nusselt number decreased by 0.76 at a 1% volume fraction of nanofluids.

Wan and J. Coney [12] examined both large and small annular space gaps at radius ratios of 0.8 and 0.955, and together they identified the components of heat transmission and their transformations. The Nusselt number showed a reasonable increase at the beginning of vortex flow and its greater transitions. At larger Taylor numbers, which equal 106, the change to periodic turbulent vortex movement also began to manifest itself in a clear change in the Nusselt number.

Khouzestani and Ghafouri [13] employed Al_2O_3 and the numerical analysis to examine the flow and heat transfer parameters for two different plump spiral center plates fixed to double pipes. The in-line configuration shape performs better than the shape with the layout, according to numerical findings. The in-line arrangement significantly improves convection heat transfer by 47.3% as compared to a smooth spiral central plate with standard flow. Utilizing nanofluids improved the thermal distribution of the wall and resulted in good thermal conductivity with minimal viscosity rise.

Lopez et al. [14] investigated the ability of working fluid to transfer heat between heated rotating and cooled fixed cylinders. The cylinders were assumed to be infinite in length, and heat transmission in the laminar regime occurs by conduction. The impacts of the geometric parameters were investigated by varying the radius ratio, length-to-gap aspect ratio, and a wide range of Prandtl, Rayleigh, and Reynolds numbers. It was discovered that the Prandtl number has no effect on the coefficient. In terms of Reynolds number, it was strong even outside of the laminar regime.

The heat transfer coefficients of benzene in a spiral flow heat exchanger were studied by Saravanan and Rajavel [15]. In the studies, different cold working fluid properties were examined, including pressure, temperature, and mass flow rate. In addition, a new connection for the Nusselt number was presented, which has a wide range of applications.

Firatoglu et al. [16] investigated experimentally and numerically the effect of horseshoe vortex (HV) legs on the circular cylinder wall heat transfer in the turbulent boundary layer of the downstream layer. It was discovered that the downstream flat surface of the circular cylinder-wall junction increased Stanton number by as much as 43%. The characteristics of deteriorating-force convective heat transfer with swirling flows in the condition of turbulent flow in a concentric annulus were modeled by Jawarneh [17]. Thermal boundary conditions were described as an adiabatically heated inner wall and an external wall. According to the simulation results, there was a clear relationship between the inlet swirl number and the heat transfer characteristics.

Palanisamy and Kumar [18] employed MWCNT nanofluid concentrations of 0.1%, 0.3%, and 0.5% to be capable of tesingt the heat transfer with the pressure gradient of a conical spiral tube heat exchanger. The tests used experimental Nusselt numbers that were 28%, 52%, and 68% greater than the equivalent nanofluid concentrations of 0.1%, 0.3%, and 0.5%. Researchers have found that the pressure gradient of nanofluids with concentrations of 0.1%, 0.3%, and 0.5% is, respectively, 16%, 30%, and 42% higher than that of water. Keawkamrop et al. [19] performed an experimental investigation to determine the effective performance of curvy spiral fin-and-tube heat exchangers at Reynolds numbers between 1500 and 6400. The results showed that the pitch or outer diameter of the fin had no visible effect on the Nusselt number or Colburn factor. However, the outcomes demonstrated that the friction factor is strongly influenced by the fin's pitch or outside diameter. A spiral heat exchanger's performance and potential uses were simulated by Khorshidi and Heidari [20].

The key equations were used to construct a lab-sized prototype of this kind of heat exchanger. The primary equation that characterized heat transmission in heat exchangers was evaluated negatively. Nusselt number increased as the mass flow rate rose. The typical Nusselt value was approximately 100, which is perfectly acceptable.

According to Liu's [21] research, Taylor vortex flow was significantly affected by a constant temperature that dropped in the plain with slot wall models. The outcomes of the theoretical and practical studies were appropriately compared. The 12-slot prototype was found to have the highest heat flux value and the best ability to transmit heat.

Kumar and Chandrasekar [22] investigated the pressure gradient and heat transfer of the conical spiral tube heat exchanger handling MWCNT nanofluids using the simulation tool ANSYS 14.5 edition. The rate of heat transmission and pressure decrease are shown to be inversely proportional to the volume concentration of MWCNT nanofluids. It is found that 0,6% MWCNT nanofluids have

pressure drop values that are 11% higher than nanofluids and Nusselt numbers that are 30% higher than nanofluids at Dean number values of 1400 and 2200, respectively. The addition of nanoparticles improved the heat transfer rate of the base fluid, and this enhancement developed continuously as the concentration increased, reaching its maximum level at the highest volume concentration [23-27].

In contrast, the effectiveness of the parameters and heat transfer coefficient of nanofluids in a double tube heat exchanger with turbulent flow was examined by Aghayari [28]. It has been found that the heat transfer coefficient increased significantly by 8% to 10%. It was discovered that as processing temperatures and/or particle concentrations rose, so did the overall heat transfer coefficient.

Zarko [29] studied the nano-Al particles in flexible burn and shock pipes. A certain oddity in the heat transport characteristics between mineral nanoparticles and a gaseous medium was carefully observed. It was discovered that the nanoparticles were enhanced to be thermally insulated from the surrounding gas medium at high temperatures and pressures. According to experimental findings, Taylor vortex flow exhibits an incredibly active flow [29, 30]. While the amount of heat transfer significantly increased as a result of spiral flow [31-37].

The information above suggests that no attempt has been made to increase heat transmission by using more than one approach simultaneously. The main objective of the current work is to enhance the functionality of the heat exchanger, which was created and used by Hashim et al. [10]. By increasing the heat exchange surface area, as well as by generating turbulence, the effect of the boundary layer can be eliminated. The last was achieved by doing the following:

1. Replacing a slot on the cylinder's outer surface with a helical fin shape between the outer and middle cylinders to be able to produce an infinite spiral flow rather than a finite swirl flow.
2. Using a suitable nanofluid with high heat conductivity, such as Al_2O_3, rather than water as a hot fluid.

RESEARCH METHODOLOGY

Experimental Setup

Figures 1 and 2 display an experimental apparatus schematic diagram. The device was made up of three concentrically positioned cylinders and an annular heat exchanger. It was designed to keep the outer and middle cylinders securely stationary, whereas the internal cylinders were attached to the belt that moves and drives it with the 0.3 hp DC motor that powers it. The diameters of the outer, middle, and inner cylinders were designed at 0.0893m, 0.0593m, and 0.185 m, respectively. The inner diameters of the outer and middle cylinders were 0.178 and 0.0838 m. The heat exchanger length for all cylinders was 1.25 m. In order to create Taylor vortices in the hot flow nanofluid, the radius ratio was utilized, N = 0.8, where the radius ratio is the ratio of the outer inner cylinder divided by the inner middle cylinder of the interior annular space. To reduce the required horsepower for rotating the cylinder, the aluminum internal cylinder was designed as a flat-faced hollow shaft. However, the central cylinder was made from nanoaluminum to achieve high thermal conductivity. It was fixed with a heat-insulating material on the middle cylinder (epoxy) and an aluminum helical shape with a pitch of 18 mm and a width of 1 mm distributed evenly to achieve infinite spiral flow rather than finite swirl flow generated in the annular space enclosed by the inner diameter of the outer cylinder and the external diameter of the middle cylinder and to avoid the fin behavior of the spiral shape. The external annular space enclosed by the outer and middle cylinders must be conducive to developing the necessary spiral flow when the fluid passes through the area, as shown in Figure 3. It should be noted that the external cylinder

Figure 1. Experimental apparatus.

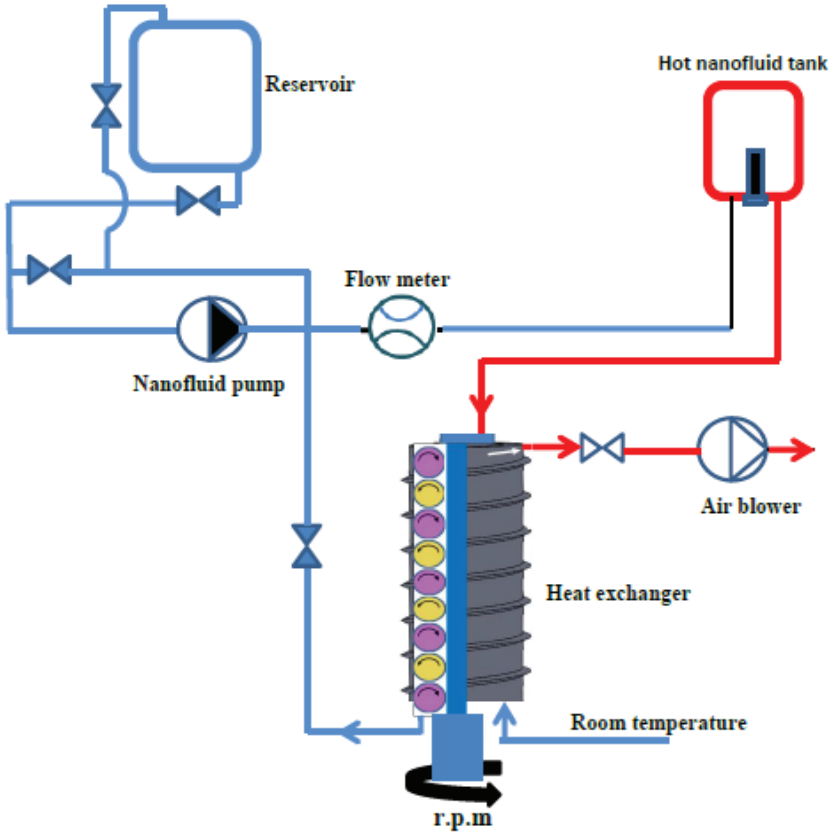

Figure 2. Schematic diagram of experimental apparatus.

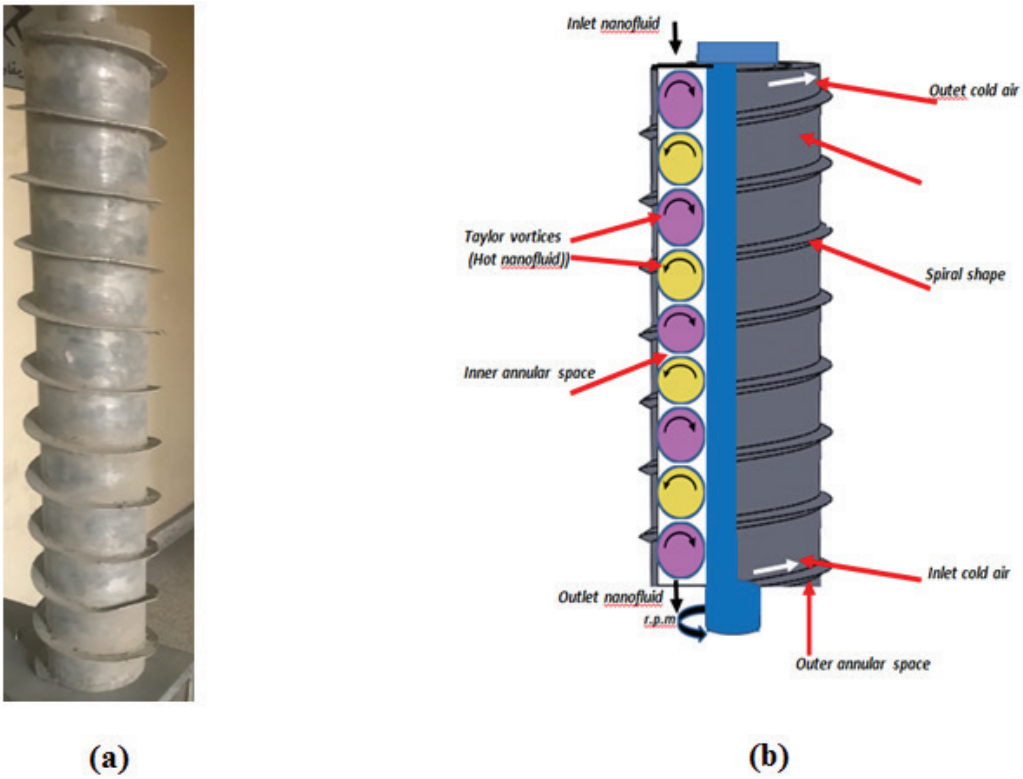

Figure 3. (a) Heat exchanger, (b) Heat exchanger cross section.

was manufactured of adiabatic Perspex metal to minimize heat losses from the system.

Two electrical heaters with 6000 W were used to heat up the nanofluid. Hot nanofluid was fed through the isolated pipe grid with an internal diameter of 12.5 mm to minimize heat losses from the pipe network and achieve steady-state heat transfer as much as feasible. A 0.5-hp centrifugal pump was also used to circulate hot nanofluid throughout the system.

On the other hand, a spiral flow was created in the outer circular space using a blower with 10 horsepower. Ball valves were utilized in both conduits to achieve a variable flow rate for hot and cold working fluids. A flow meter, type ball, is employed to monitor the flow rate of hot nan-fluid. A vane anemometer with a digital signal was also used to record the flow rate of cold working fluid (air). A thermocouple type K and a digital signal thermometer were used to measure the entrance and output temperatures for both non-fluid and air. It is worth mentioning that the inner cylinder's rotational speed was determined using a laser tachometer.

Nanomaterial Thermo-Physical Properties

The present work employed the well-established and reliable method of electric explosion of wires to produce reasonable and reactive powders, namely nano-aluminum powders. Small fractions of the nanofluids, including metallic particles, were studied in previous experimental research. However, it is unclear if the heat conductivity is affected by the particle size. As a result, the findings might be related to the base fluid's and the solid's bulk thermal conductivities. Three sizes of nanoparticles were examined to ascertain the thermal conductivity of aluminum powder nanofluids. Eq. (1) was used to fit the data from the literature for metallic nanoparticle-rich nanofluids, both with and without accounting for the thermal conductivity of the particles' volume dependence [25].

$$(k_{eff})^n = (k_p)^n \phi + (k_l)^n (1 - \phi) - 1 < n < 1 \quad (1)$$

Nanofluids Thermo-Physical Properties

The density, thermal conductivity, specific heat, and viscosity of nanofluids have all been calculated using Eqs. (2), (3), (4), and (5) since the mathematical conclusions are more precise than the experimental data [17]. The dry water and Al_2O_3 properties used in these tests are listed in Table 1 [38].

$$\rho_{nf} = \varphi\rho_p + (1 - \varphi)\rho_w \quad (2)$$

$$(\rho c_p)_{nf} = (1 - \varphi)(\rho c_p) + \varphi(\rho c_p)_s \quad (3)$$

$$k_{nf} = k_f \left[1 + \frac{k_p \varphi r_f}{k_f (1 - \varphi) r_p}\right] \quad (4)$$

$$\mu_{nf} = \mu_f (1 + 22.7814\varphi - 9748.4\varphi^2 + 1000000\varphi^3) \quad (5)$$

Table 1. Al_2O_3-Water nanofluid thermo-physical properties [38]

Material	ρ kg/m³	Cp J/(Kg·K)	k W/(m. K)	μ Kg /(m·s)
Pure water c = 0%	981.3	4189	0.643	0.000598
Al_2O_3-water c = 5%	1112.2	4017.8	0.739	0.000672

Modeling

The analysis was predicated on the following premises:

1. Heat loses to the environment are neglected.
2. Assume the whole system is in a steady-state operation.
3. Hot fluid in a single phase.
4. The capacity of hot and cold fluids is constant.
5. The overall heat transfer coefficient is constant.

The equations below were used to determine the heat exchanger's longitudinal Reynolds number and the number of thermal transfer units for both nanofluid and air [39-44].

$$NTU = \frac{AU}{C_{min}} = \frac{q}{LMTD.C_{min}} \quad (6)$$

$$q = m_{nf}.Cp_{nf}.\Delta T_{nf} = m_A.Cp_A.\Delta T_A \quad (7)$$

$$LMTD = \frac{\Delta T_1 - \Delta T_2}{ln\frac{\Delta T_1}{\Delta T_2}} \quad (8)$$

$$Re_{nf} = \frac{u_{nf}(2C_1)}{\vartheta_{nf}} \quad (9)$$

$$Re_A = \frac{u_A(2C_2)}{\vartheta_A} \quad (10)$$

$$\varepsilon = \frac{m_A Cp_A(T_{A2} - T_{A1})}{C_{min}(T_{nf1} - T_{A1})} = \frac{T_{A2} - T_{A1}}{T_{nf1} - T_{A1}} \quad (11)$$

Eq. (12) can be used to calculate Taylor's number of nanofluids from the inner cylinder's angular velocity, the inner diameter of the middle cylinder, and the outer radius of the inner cylinder.

$$T_a = \frac{2\omega_1^2 R_1^2 C_1^3}{(R_1 + R_2)\vartheta_{nf}^2} \quad (12)$$

$$EPR\% = \frac{\varepsilon_{nanofluid\ with\ spiral\ flow} - \varepsilon_{water\ with\ swirl\ flow}}{\varepsilon_{nanofluid\ with\ spiral\ flow}} \times 100\% \quad (13)$$

RESULTS AND DISCUSSION

Taylor vortex flow of hot, nano-fluid Al_2O_3 with 0.5% volume concentrations was studied in the current study. According to Hashim et al. [10], air and infinite spiral flow are generated in a heat exchanger with counter flow in place of water and finite swirl flow. Taylor vortices were created in the inside cylinder while remaining stationary in the outer cylinder by heating nanofluid to 80°C in the annular space between the overlapping cylinders. The first annular of the inner cylinder surrounds the outer annular, which was separated from it by a high-conductivity metal, and produces a helical spiral flow for cold working fluid (air) at ambient temperature (bulk aluminum nanoparticles). At different flow rates, the heat transfer of the wall between the Taylor vortex and spiral flow was also determined.

In order to assess the efficacy of the heat exchanger, analysis and measurements of the air and nanofluid inlet and outlet temperatures were made when the vortex started to degrade approaching the heat exchanger's exit. The efficiency and number of transfer units (NTU) of the heat exchanger can be calculated as a result. The present work used the rotating speed of the internal hollow shaft of 80 r.p.m. for the flow rates of hot nanofluid and cold air of 2.61, 2.69, 2.72, 2.92, 2.94, 2.97, 3.02, 3.03, and 3.03* 10^{-2} m^3/s, respectively. The variation of the number transfer unit with cold air flow rates at constant hot nanofluid flow rates and internal cylinder rotational speed is shown in Figure 4. It is clear that the heat transfer value increases with the rate of the cold air flow until it reaches its peak value of 0.74. After that, the heat transfer value decreases, which was

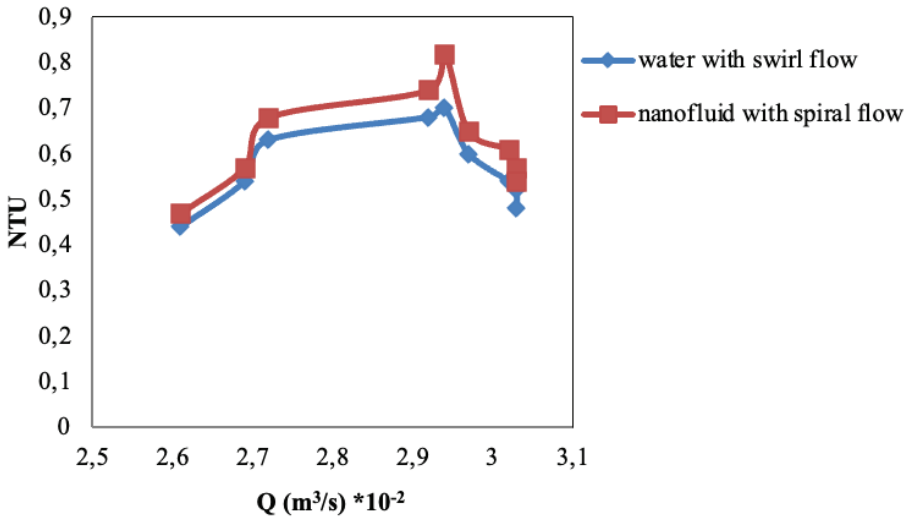

Figure 4. Variation of number transfer unit with cold air flow rates (Re_{nf}=2313).

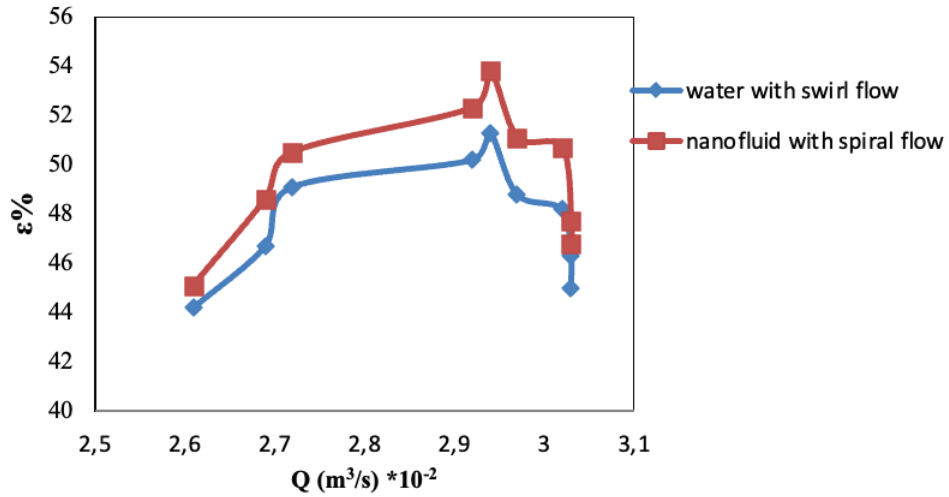

Figure 5. Variation of the effectiveness with cold air flow rate.

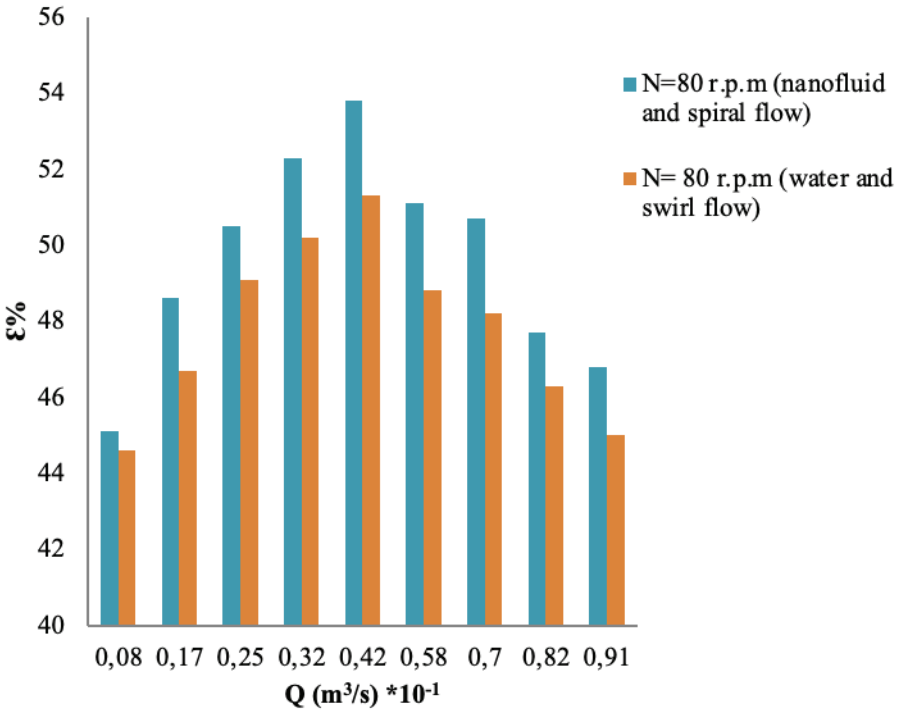

Figure 6. Variation of the effectiveness with and withot nanofluid and spiral flow at different cold air flow rate.

related to a lack of time for the heat exchange between the hot surface of the cylinder and the cold air. It seems that the heat exchanger under study is superior to that in the previous study [10] for all values of cold air flow rate because the use of nanofluid increases the thermal conductivity of the hot fluid. Figure 4 also shows a good comparison between the usage of hot water with a nanofluid and the finite swirl flow with the infinite spiral flow of cold air, where the continuous spiral flow exhibits more effectiveness. In effect, the swirl vortex that is created by the slots on the outer cylinder walls decays at a given distance and has a significant effect on reducing the heat in the hot fluid.

Figures 5 and 6 displays the variation of the heat exchanger efficiency at a constant inner cylinder speed of 80 r.p.m with a flow rate of cold air at room temperature. It is evident that the effectiveness of the heat exchangers grows with air flow rates until reaching the maximum value of 53.8. Whereas, the effectiveness of heat exchangers starts to decline as the flow rate increases because some fluids do not have enough fluid surface area to exchange heat with. It is evident that the effectiveness of the heat exchanger under examination is clearly superior at all flow rate values.

Taylor vortices that were generated in the heated fluid (nanofluid) and spiral flow of the cooled fluid (air) at the inner cylinder speed of 80 r.p.m instead of water are shown in Figure 7. It should be noted that the working fluid's higher conductivity and prevention of the flow decaying phenomenon in swirl flow led to an increase in the enhancement percentage ratio (EPR) of heat exchanger effectiveness.

The effectiveness recorded for the flow rates (2.61, 2.69, 2.72, 2.92, 2.94, 2.97, 3.02, 3.03, and 3.03* 10^{-2}) m^3/s was 1.1% and 3.9%, 2.8%, 4%, 4.6%, 4.5%, 4.9%, 2.9%, and 3.8%, respectively. It is clear to notice that the maximum percentage obtained does not necessarily represent the highest heat exchanger efficiency under study.

The tested heat exchanger showed the highest efficiency at a flow rate of 2.94×10^{-2} m^3/s, while the comparative heat exchanger showed the largest percentage increase at 3.022×10^{-2} m^3/s. The height of the swirl flow cavity affects the efficiency of heat exchange because it reduces the flow velocity. This reduces the amount of heat exchanged between the two working fluids in the heat exchanger. Heat transfer is improved when boundary layers do not integrate due to the increased flow rate concentration adjacent to the walls due to swirl-induced cross-flow and entrainment.

The exchanger under investigation was compared with the typical heat exchanger that is created in accordance with international standards. The behavior of the standard heat exchanger with the opposite linear flow of fluids is shown in Figure 8. It is clear to see that the heat exchanger's efficiency drastically dropped in order to raise the C_{min}/C_{max} ratio, which measures the heat exchange fluids' minimum and highest thermal contents. The points a and b show the performance of the exchanger when it was tested at an internal cylinder speed of 80 r.p.m and the ratio (C_{min}/C_{max}).

The points in Table 2 are situated on the behavior curve at the ratio (C_{min}/C_{max}), as seen in Figure 8. This suggests that the exchanger's efficiency at this proportion

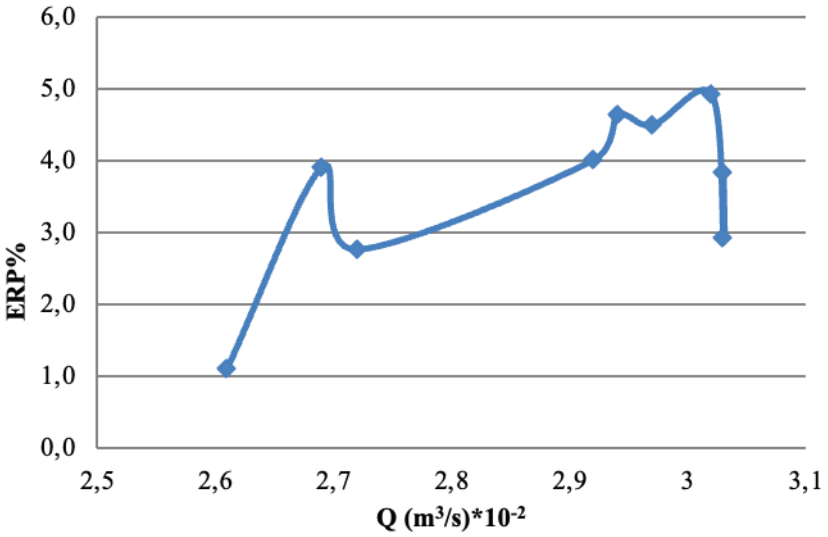

Figure 7. Variation of the enhancement ratio percentage with different cold air flow rate.

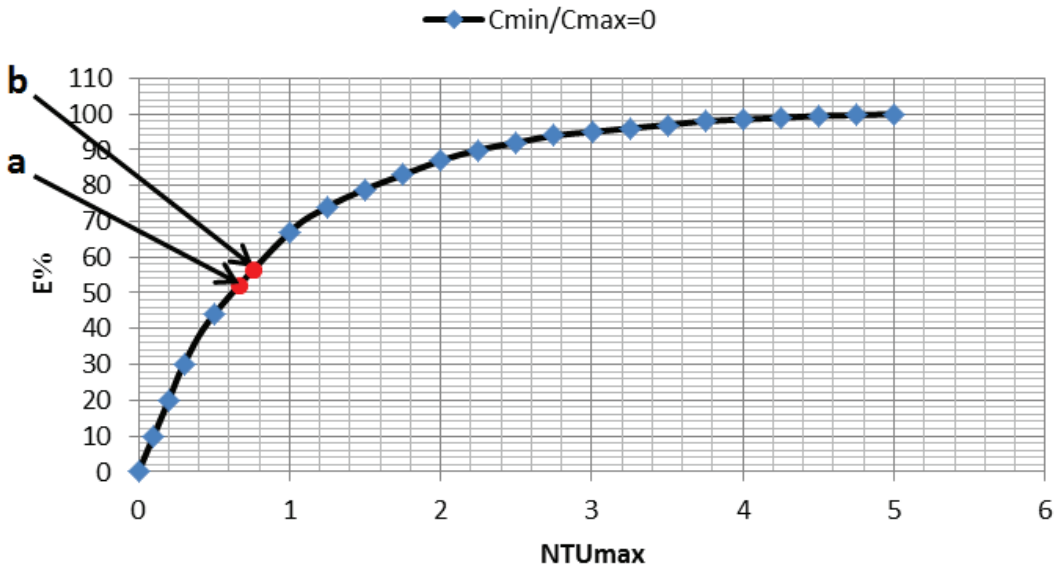

Figure 8. The standard exchanger performance.

Table 2. Points property

Point	Renf	Rea	N (r.p.m)	Ta	NTU	ε%
a	2135	8760	80	1.76E4	0.7086	51.3
b	2313	8760	80	1.79 E4	0.8202	53.8

($C_{min}/C_{max} = 0.08$) could be improved over the exchanger's efficiency as a ratio ($C_{min}/C_{max} = 0$). The better criteria to achieve the best results is superior performance by using spiral low and nanofluids in the heat exchange, which helps to avoid swirl flow decay as well as increase the thermal conductivity of the hot working fluid.

For the reasons listed below, the present technique has performed better than earlier ones:

1. The two strategies of increasing heat transfer using vortices and infinite spiral flow were combined in the current study rather than being employed independently as in earlier investigations.

2. Using nano-aluminum as a heat transfer medium instead of regular aluminum to increase thermal conductivity
3. Using nanofluid as a hot fluid instead of water to increase thermal conductivity.

CONCLUSION

In this study the enhancement of heat exchanger performance by using hot nanofluid and adaption of the infinite spiral flow instead of water and finite swirl have been investigated. The following conclusions have been deduced:

1- The conventional heat exchanger and improved heat exchanger exhibit a higher level at the same ratio (C_{min}/C_{max} = 0) than that in the current heat exchanger at the ratio (C_{min}/C_{max} = 0.08).

2- The highest efficiency was observed in the current heat exchanger, due to the use of nanofluid instead of water as a hot fluid, while infinite spiral flow was used as an alternative to the finite flow of cold air.

3- The heat exchanger efficiency is thought to be positively impacted by the values of the Taylor number and cold air flow rate, which are 3.022* 10-2 m^3/s. The effectiveness increased noticeably from 51.3% to 53.8% as the Taylor number rose from zero to 1.79 E4.

4- It was established that the greatest enhancement percentage ratio (EPR) found did not necessarily reflect the heat exchanger under study's highest level of efficiency

In summary, it could be concluded that current heat exchanger's higher performance might make it possible to reduce its surface area and, in turn, the size of a specific application. Hence, it was suggested to correlate the theoretical analysis by using CFD program with simulation of the flow and heat transfer inside a heat exchanger. On the other hand, determining the Nusselt number involves monitoring the surface temperatures at several sites along the heat exchanger that are spaced equally apart and determining the difference between the amount of heat gained and lost.

NOMENCLATURE

A	Heat transfer area (m^2)
c	Concentration
C_p	Specific heat capacity J/(Kg•K)
EPR	Enhancement percentage ratio
k	Thermal conductivity($W/m^2.K$)
k_{eff}	Effective thermal conductivity($W/m^2.K$)
k_p	Thermal conductivity of the particles
LMTD	Logarithm mean temperature difference (°C)
m	Nanofhuid mass flow rate (m^3/s)
n	Index
N1	Radius ratio of internal annular space
NTU	Number of Transfer Unit
Q	Internal cylinder speed (r.p.m)
q	Heat transfer rate (W)
R_1	Outer radius of internal cylinder (m)
R_2	Inner radius of middle cylinder (m)
Re	Reynolds number
T	Temperature (°C)
Ta	Taylor number
ΔT	Temperature difference (°C)
Ta	Taylor number
Ta_c	Critical Taylor number
u	Velocity (m/s)
U	Overall heat transfer coefficient ($W/ m^2.K$)

Greek symbols

ε	Heat exchanger effectiveness
ω_1	Angular velocity of internal cylinder (rad/s)
ν	Kinematic viscosity (m^2/s)
Γ	Length to gap aspect ratio
ϕ	Volume concentration
φ	Volume fraction
ρ	Density (kg/m^3)
μ	dynamic viscosity (kg /m•s)
η	radius ratio

Subscripts

A	Air
f	Fluid
nf	Nanofluid
p	particles
s	Solid
w	Water
1	Heat exchanger inlet
2	Heat exchanger outlet

AUTHORSHIP CONTRIBUTIONS

Authors equally contributed to this work.

DATA AVAILABILITY STATEMENT

The authors confirm that the data that supports the findings of this study are available within the article. Raw data that support the finding of this study are available from the corresponding author, upon reasonable request.

CONFLICT OF INTEREST

The authors declared no potential conflicts of interest with respect to the research, authorship, and/or publication of this article.

ETHICS

There are no ethical issues with the publication of this manuscript.

REFERENCES

[1] Ramadhan AA. Numerical study of fluid flow and heat transfer over a bank of ovaltubes heat exchanger with vortex generators. Anbar J Eng Sci 2012;5:88–107. [CrossRef]

[2] Yang KS, Zheng JW, Wu KL, Wu YL. Performance of the frosting characteristics of fin-and-tube heat exchanger subject to superhydrophobic coating. Appl Therm Eng J 2023;235:121338. [CrossRef]
[3] Varkaneh AS, Nooshabadi GA, Arani AA. Flow field and heat transfer of ferromagnetic nanofluid in presence of magnetic field inside a corrugated tube. J Therm Eng 2023;9:1667−1686. [CrossRef]
[4] Basiri M, Goshayeshi HR, Chaer I, Pourpasha H, Heris SZ. Experimental study on heat transfer from rectangular fins in combined convection. J Therm Eng 2023;9:1632−1642. [CrossRef]
[5] Barati E, Zarkak M, Jalali S. Analysis of heat transfer and flow over a rotating cylinder at subcritical Reynolds numbers based on Taguchi method. J Therm Eng 2023;9:998−1014. [CrossRef]
[6] Eiamsa S, Ploychay Y, Sripattanapipat S, Promvong P. An experimental study of heat transfer and friction factor characteristics in a circular tube fitted with a helical tape. Proceedings of 18th Conf. of Mechanical Engineering Network of Thailand, 18-20 October 2004.
[7] Kidd GJ Jr. The heat transfer and pressure-drop characteristics of gas flow inside spirally corrugated tubes. J. Heat Transfer 1970;92:513−519. [CrossRef]
[8] Guo Z, Dhir V. Single and two-phase heat transfer in tangential injection-induced swirl flow. Int J Heat Fluid Flow 1989;10:203−210. [CrossRef]
[9] Garimella S, Richards D, Christensen R. Experimental investigation of heat transfer in coiled annular ducts. J Heat Transf 1988;2:329−336. [CrossRef]
[10] Hashim WM, Hoshi HA, Al-Salihi HA. Enhancement the performance of swirl heat exchanger by using vortices and nanoaluminume. Heliyon 2019;5:e02268. [CrossRef]
[11] Onyiriuka EJ, Ighodaro OO, Adelaja AO, Ewim DRE, Bhattacharyya S. A numerical investigation of the heat transfer characteristics of water-based mango bark nanofluid flowing in a double-pipe heat exchanger. Heliyon 2019;5:e02416. [CrossRef]
[12] Wan C, Coney J. An experimental study of diabatic spiral vortex flow. Int J Heat Fluid Flow1982;3:31−38. [CrossRef]
[13] Khouzestani RF, Ghafouri A. Numerical study on heat transfer and nanofluid flow in pipes fitted with different dimpled spiral center plate. SN Appl Sci 2020;2:298. [CrossRef]
[14] Lopez J, Marques F, Avila M. Conductive and convective heat transfer in fluid flows between differentially heated and rotating cylinders. Int J Heat Mass Transf 2015;90:959−967. [CrossRef]
[15] Saravanan K, Rajavel R. Analysis of heat transfer enhancement in spiral plate heat exchanger. Mod Appl Sci 2008;2:4. [CrossRef]
[16] Firatoglu ZA, Yemenici O, Umur H. Experimental and numerical investigation of the effect of horseshoe vortex legs on heat characteristics of the downstream region of a circular cylinder-wall junction. Int J Heat Mass Transf 2021;180:121726. [CrossRef]
[17] Jawraneh A. Heat transfer enhancement in swirl annulus flows. Proceedings of 5th WSEAS Int. Conf. on Environment, Ecosystems and Development, Tenerife, Spain, 14-16 December 2007.
[18] Palanisamy K, Kumar PCM. Experimental investigation on convective heat transfer and pressure drop of cone helically coiled tube heat exchanger using carbon nanotubes/ nanofhuid. Heliyon 2019;5:e01705. [CrossRef]
[19] Keawkamrop T, Asirvatham LG, Dalkılıç AS, Ahn HS, Mahian O, Wongwises S. An experimental investigation of the air-side performance of crimped spiral fin-and-tube heat exchangers with a small tube diameter. Int J Heat Mass Transf 2021;178:121571. [CrossRef]
[20] Khorshidi J, Heidari S. Design and construction of a spiral heat exchanger. Adv Chem Eng Sci 2016;6:201−208. [CrossRef]
[21] Liu D, Wang YZ, Shi WD, Kim HB, Tang AK. Slit wall and heat transfer effect on the taylor vortex flow. Energies 2015;8:1958−1974. [CrossRef]
[22] Kumar PCM, Chandrasekar M. CFD analysis on heat and flow characteristics of double helically coiled tube heat exchanger handling MWCNT/ nanofluids. Heliyon 2019;5:e02030. [CrossRef]
[23] Kamila S, Venu Gopal VR. Acoustics and thermal studies of conventional heat transfer fluids mixed with ZnO nano flakes at different temperatures. Heliyon 2019;5:e02445. [CrossRef]
[24] Askar AH, Kadhim SA, Mshehid SH. The surfactants effect on the heat transfer enhancement and stability of nanofluid at constant wall temperature. Heliyon 2020;6:e04419. [CrossRef]
[25] Ali SA, Ekaid L, Ibrahim SH, Alesbe I. Mixed convection in sinusoidal lid driven cavity with non-uniform temperature distribution on the wall utilizing nanofluid. Heliyon 2021;7:e06907. [CrossRef]
[26] Hirpho M, Ibrahim W. Dynamics of flow in trapezoidal enclosure having a heated inner circular cylinder containing Casson nanofluid. Heliyonl 2021;7:e07683. [CrossRef]
[27] Najim S, Hussein A, Danook SH. Performance improvement of shell and tube heat exchanger by using Fe3O4/water nanofluid. J Therm Eng 2023;9:24−32. [CrossRef]
[28] Aghayari R, Madah H, Keyvani B, Moghadassi A, Ashori F. The effect of nanoparticles on thermal efficiency of double tube heat exchangers in turbulent flow. ISRN Mechanical Eng 2014;274560. [CrossRef]
[29] Zarko W. Effect of heat transfer peculiarities on ignition and combustion behavior of al nanoparticles. Euras Chem Tech J 2016;8:ectj423. [CrossRef]

[30] Kostein L, Finat Y. Investigation of heat transfer of a turbulent flow of air in an annular gap between rotating coaxial cylinders. Ivzh FIZ Zh 1963;8:3–9. [CrossRef]

[31] Modena MC, González LM, Valero E. Numerical optimization of the fin shape experiments of a heat conjugate problem surface air/oil heat exchanger (SACOC). Int J Heat Mass Transf 2022;182:121971. [CrossRef]

[32] Niroom R, Saidi MH, Hannani SK. A new multi-scale modeling framework for investigating thermally-induced flow maldistribution in multi-stream plate-fin heat exchangers. Int J Heat Mass Transf 2021;180:121779. [CrossRef]

[33] Ziyong L, Ling CS, Zhang Z. Experimental and numerical investigation on flow and heat transfer characteristics of a multi-waves internally spiral finned tube. Int J Heat Mass Transf 2021;172:121104. [CrossRef]

[34] Zhongyang Y, Leren T, Lihaoa H, Dong W. Numerical investigation on cooling heat transfer and flow characteristic of supercritical CO2 in spirally fluted tubes. Int J Heat Mass Transf 2020;163:120399. [CrossRef]

[35] Cong XZ, Pan QY, Liang T. Effects of screw pitches and rotation angles on flow and heat transfer characteristics of nanofluids in spiral tubes. Int J Heat Mass Transf 2019;130:989–1003. [CrossRef]

[36] Tang X, Dai XF, Zhu D. Experimental and numerical investigation of convective heat transfer and fluid flow in twisted spiral tube. Int J Heat Mass Transf 2015;90:523–541. [CrossRef]

[37] Neeraas BO, Fredheim AO, Aunan B. Experimental data and model for heat transfer, in liquid falling film flow on shell-side, for spiral-wound LNG heat exchanger. Int J Heat Mass Transf 2004;47:3565–3572. [CrossRef]

[38] Warrier P, Teja A. Effect of particle size on the thermal conductivity of nanofluids containing metallic nanoparticles. Nanoscale Res Lett 2011;6:247. [CrossRef]

[39] Mujtaba HS, Feroze T, Hananni A, Shams HA. A CFD investigation of the design variables affecting the performance of finned-tube heat exchangers. J Therm Eng 2023;9:1041−1052. [CrossRef]

[40] Taylor G. Stability of a viscous liquid contained between two rotating cylinders. JSTOR 1923;223:289−343. [CrossRef]

[41] Koschmieder EL. Bénard Cells and Taylor Vortices. UK: Cambridge University Press; 1993.

[42] Hasan MI, Muhsin AA. Rageb MY. Investigation of a counter flow microchannel heat exchanger performance with using nanofluid as a coolant. J Electr Cool Therm Cont 2012;2:35−43. [CrossRef]

[43] Holman JP. Heat Transfer. 10th ed. New York: McGraw-Hill; 2006.

[44] White M. Fluid Mechanics. 7th ed. New York: McGraw-Hill 2009.